

Estimation of the Thickness of the Lunar Uppermost Basalt Layer Based on Lunar Radar Sounder Observations

Chenyang Zhang , Gang Wan, Lei Liu, and Yutong Jia 

Abstract—Research on lunar basalt thickness and subsurface features is of great significance to conclude the magma evolution history and explore the thermal evolution process of the Moon. The mission of Lunar Radar Sounder (LRS) made subsurface detection within all major lunar maria. Nevertheless, determining the actual depth of reflector needs to estimate the dielectric constants of the uppermost basalt layer. In this article, we use Maxwell-Garnett theory to determine the unique dielectric constant values of the fifth oldest unit in Mare Humorum (unit H5) and use the two-layer model to calculate the basalt layer thickness. The result shows that the thickness of basalt in the upper layer of unit H5 is 180 m and 120 m at the border between unit H5 and H7. It points out that the basalt in adjacent units may intrude below the boundary of unit H5.

Index Terms—Bulk dielectric constant, lunar radar sounder (LRS), moon, subsurface reflector.

I. INTRODUCTION

THE lunar maria are composed of basalts rich in titanium and iron that were generated mainly by volcanism. [1]. The volume of lunar mare basalts is of great scientific significance, because it can constrain the thermal evolution of the Moon. The volume of lunar mare basalts can be estimated as the product of surface area and thickness. The surface area of maria has been estimated in previous research [2]. Radar measurement of basalt thickness is very mature now. The Lunar Radar Sounder (LRS) onboard Kaguya (SELENE) provides the echo data of the discontinuous reflector under all major lunar maria and helps reveal the formation and evolution of the Moon by investigating the stratigraphic and crustal tectonic features of the Moon's underground [3]. The subsurface reflector is the boundary between the maria basalt layers. The sudden changes in the dielectric constant of different basalt layers produce echoes in radar detection. By estimating the depth of the reflector, we can get the thickness of the basalt layer [4].

However, analysis of the reflector requires the determination of the dielectric constant inside the Moon. The propagation

distance of radar waves in the vacuum is called apparent distance. When the propagation medium becomes the subsurface layer of the Moon, the apparent distance needs to be divided by the square root of the dielectric constant of the medium. Suppose the speed of light in a vacuum is c . In that case, the dielectric constant of the lunar subsurface is $\varepsilon_{\text{bulk}}$, and the time difference between the subsurface and surface echoes is Δt . The formula can obtain the actual depth of the subsurface reflector

$$d = \frac{c}{\sqrt{\varepsilon_{\text{bulk}}}} \cdot \frac{\Delta t}{2}. \quad (1)$$

Three methods have been used to determine dielectric constants in past lunar radar observations: 1) A reasonable dielectric constant is assumed based on the Apollo basalt samples measured on the ground [5]–[7]. 2) Researchers use particular physical models based on different datasets obtained by optical and radar remote sensing to determine the bulk dielectric constant [8], [9]. 3) Estimating the bulk dielectric constant by using the strong correlation between density and dielectric constant of basalt [10], [11]. The first method directly assumes the dielectric constant without considering the spatial distribution of the dielectric constant, and the results obtained are biased. The second method relies on the unique lunar terrain and can only be used for dielectric constant inversion in parts of the Moon. The third method applies to highland regolith or maria basalt in most areas of the Moon.

Peeples *et al.* [5] studied the Apollo Lunar Sounder Experiment (ALSE) data, assuming that the bulk dielectric constant ε of the maria basalt is 8.7. It is concluded that there are two subsurface reflectors with average apparent depths of 0.9 and 1.6 km in Mare Serenitatis. Ono *et al.* [3] used the Fresnel model to determine the loss angle tangent of the top basalt layer and the dielectric constant and depth of two subsurface layers assuming a moderate value of 4 for the dielectric constant of the top layer. Both studies reported the presence of subsurface reflectors beneath maria. The apparent depths of these reflectors are usually several hundred meters. Since the dielectric constant of the bulk comes from assumptions, there is a significant deviation in their actual depths. Ishiyama *et al.* [8] comprehensively analyzed adjacent impact craters covering basalt sputters from different strata based on Terrain Camera (TC) and Multiband Imager (MI) data. Determine the thickness range of the uppermost basalt layer by taking the depth of the two craters as an interval. Then, the bulk dielectric constant of the uppermost

Manuscript received January 13, 2022; revised February 21, 2022 and April 19, 2022; accepted May 6, 2022. Date of publication May 10, 2022; date of current version May 19, 2022. (Corresponding author: Chenyang Zhang.)

Chenyang Zhang is with the Unit 63680 of PLA, Wuxi 214400, China (e-mail: chenyang2077@qq.com).

Gang Wan, Lei Liu, and Yutong Jia are with the School of Space Information, Space Engineering University, Beijing 101416, China (e-mail: casper_51@163.com; drliu_uavrs@163.com; 963810890@qq.com).

Digital Object Identifier 10.1109/JSTARS.2022.3173790

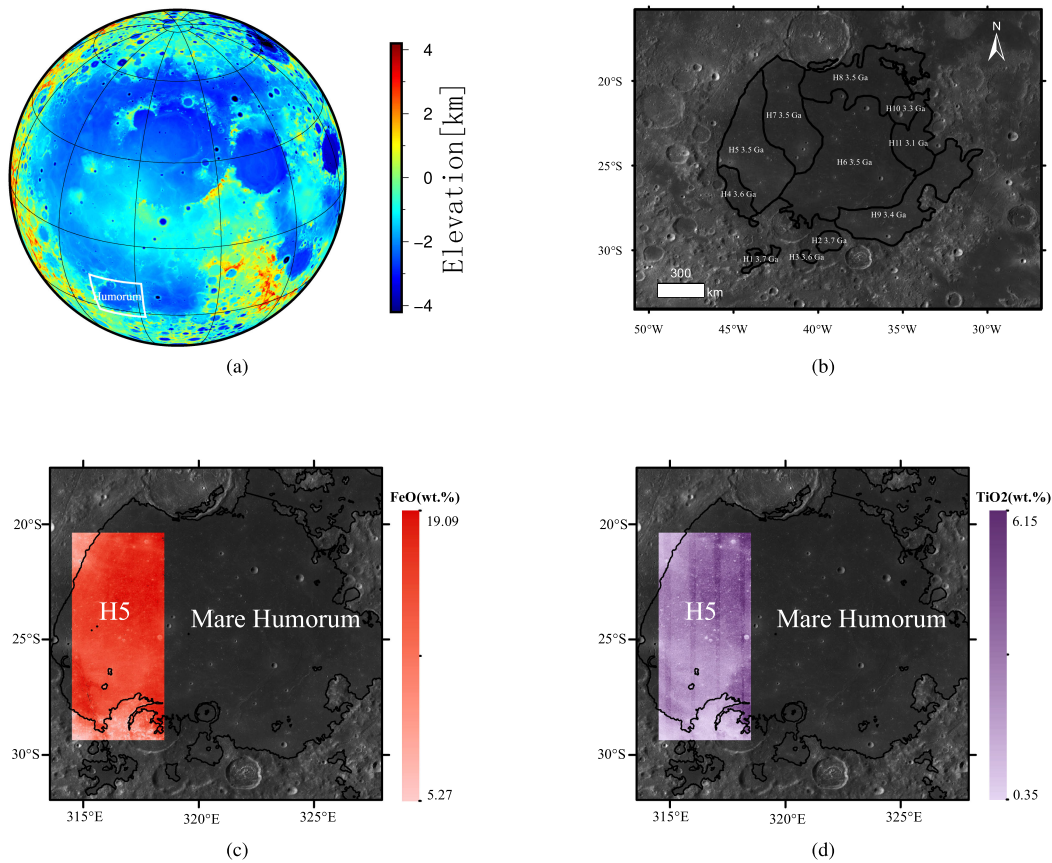


Fig. 1. (a) A topographic map showing Mare Humorum and the nearside of the Moon. (b) A Lunar Reconnaissance Orbiter Camera (LROC) Wide Angle Camera image showing the geological units in Mare Humorum. (c) and (d) FeO and TiO₂ content map of unit H5. It can be seen that the content of ilmenite in maria is higher than that in lunar highland.

basalt layer is calculated with the time delay in LRS data. Hongo determines the site-dependent bulk dielectric constants using a two-layer model consisting of a surface regolith layer over a half-space with uniform but different physical properties from the upper layer [9]. Hongo's method will cause significant errors in estimating the dielectric constant due to the surface clutter generated by the rugged surface. These two methods have strict requirements on the topography of the study area and are not suitable for generalizing the dielectric constant inversion of all maria. Fa *et al.* [11] refitted the existing dielectric constant measurements as a function of bulk density, porosity, FeO and TiO₂ abundance. They prepared the lunar soil dielectric constant map over the lunar nearside. Their predicted dielectric constant ranges from 2.5 to 3.4, which is very close to Carrier *et al.*'s estimate of 2.7–3.8 [12].

Previous studies on the thickness of basalt assumed or inverted dielectric constant is single and does not change with the longitude and latitude of the lunar surface [3], [7] [8], [9]. Such a dielectric constant is unreasonable. This article aims to calculate the spatial distribution of dielectric constants of the maria basalt using the ferrous and titanium content of the maria and the porosity and permittivity of APOLLO samples. Finally, the thickness of the uppermost basalt in unit H5 (see Fig. 1) is estimated based on LRS data. Unit H5 is the fifth oldest unit in Humorum, defined in age estimate works by Hiesinger *et al.* [13].

II. DATA DESCRIPTION

In this study, MI data and LRS data obtained by Kaguya are used for our basalt layer thickness research. These data are downloaded from the JAXA-SELENA data archive.¹

A. LRS Data

LRS is a high-frequency radar (5 MHz) designed to detect terrain features thousands of meters below the lunar surface. LRS has a pair of mutually orthogonal 30 m dipole antennas. The pulse width of LRS's transmitted chirp signals is 200 μ s. The LRS's vertical resolution in a vacuum is 75 m/pixel and in basalt varies according to the dielectric constant. The echoes collected by LRS were made into two data products, A-scope and B-scan. A-scope used LRS's raw echo power to display a plot of signal amplitude versus depth, as shown in Fig. 5. B-scan is SAR-processed radargrams, which can help identify the subsurface echoes clearly, as shown in Fig. 3.

B. MI Data

MI is a multispectral imaging camera with five visible bands (415, 750, 900, 950, and 1000 nm) and four near-infrared bands

¹[Online]. Available: <https://darts.isas.jaxa.jp/planet/pdap/selena/>

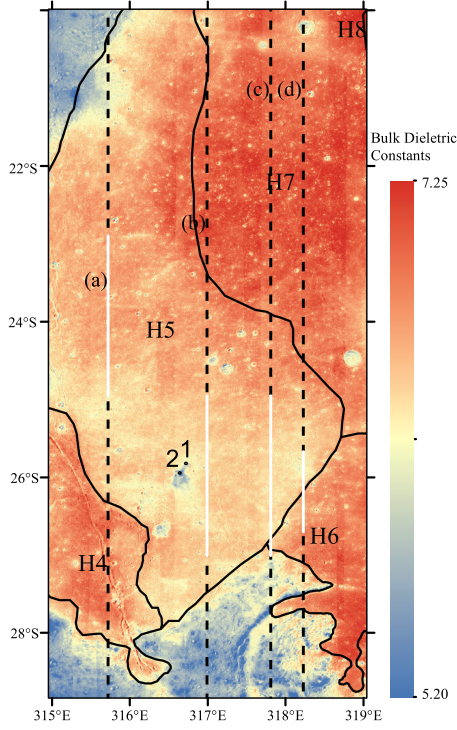


Fig. 2. Dielectric constant map in Mare Humorum. The black dotted lines of mark (a)–(d) refer to the ground tracks of LRS on unit H5, which correspond to (a)–(d) in Fig. 3. The white solid lines are reflectors selected to measure the thickness, corresponding to red double-arrows in Fig. 3. The black dots marked 1 and 2 represent two craters in Ishiyama’s study.

(1000, 1050, 1250, and 1550 nm). At Kaguya’s orbital height of 100 km, the spatial resolution of the visible band is 20 m/pixel, and that of the near-infrared band is 62 m/pixel. We can use MAP-V3.0 level data to calculate the ferrous and the titanium content of maria.

C. FeO and TiO₂ Abundance

Previous analysis of lunar basalt samples has revealed a correlation between the physical properties of the basalts [14], [15]. The loss tangent, density, and dielectric constant of lunar basalt are closely related to the content of FeO and TiO₂. However, the ferrous and titanium content of the lunar surface cannot be measured directly. Previous work generally followed or improved Lucey’s method of retrieving FeO and TiO₂ content based on Clementine UV/VIS data [16]. This article uses Lemelin’s method to retrieve FeO content [17], and Lucey’s method is used to retrieve TiO₂ content [16]. They are all based on MI data

$$\text{FeO}(\text{wt}\%) = 1.0708 \times \theta_{\text{Fe}_2} - 0.3986 \quad (2)$$

$$\theta_{\text{Fe}_2} = 0.0656e^{(3.6681 \times \theta_{\text{Fe}_1})} \quad (3)$$

$$\theta_{\text{Fe}_1} = -\arctan \frac{R_{950}/R_{750} - 1.39}{R_{750} - 0.04} \quad (4)$$

$$\text{TiO}_2(\text{wt}\%) = \theta_{\text{Ti}}^{14.964} \times 0.72 \quad (5)$$

$$\theta_{\text{Ti}} = -\arctan \frac{R_{415}/R_{750} - 0.28}{R_{750} + 0.108} \quad (6)$$

where R_{415} , R_{750} , and R_{950} represent the reflectance at 415, 750, and 950 nm, respectively. θ_{Ti} and θ_{Fe} refer to titanium-sensitive and Fe-sensitive parameters. The standard deviation of iron is 0.85 wt.%, and that of titanium is 0.43 wt.% [18].

Based on MI data, this article uses the above method to retrieve the content of titanium dioxide and iron oxide in unit H5, as shown in the Fig. 1.

III. ESTIMATION OF THE BULK PERMITTIVITY IN THE UPPERMOST BASALT

Maxwell–Garnett theory is one of the influential media theories, which allows us to treat nonuniform dielectric constant media as uniform dielectric constant media. Fa and Wiezorek used constant porosity, particle dielectric constant, and Maxwell–Garnett theory to obtain the functional relationship between dielectric constant (ϵ) and density (ρ) of lunar soil [11]. This theory can be expressed by the following formula:

$$\frac{1}{\rho_1} \cdot \frac{\epsilon_1 - 1}{\epsilon_1 + 2} = \frac{1}{\rho_2} \cdot \frac{\epsilon_2 - 1}{\epsilon_2 + 2} \quad (7)$$

where ϵ_1 and ϵ_2 are the dielectric constants of lunar soil when density is ρ_1 and ρ_2 .

A. Assuming the Porosity of Basalt Layer

Porosity n is defined as the volume of void space between particles divided by the total volume. The relationship between particle density, bulk density, and porosity is

$$\rho_{\text{bulk}} = \rho_{\text{grain}}(1 - n). \quad (8)$$

The porosity of lunar basalts is mainly from the vesicles generated when lava flow crystallizes into basalts. In addition to vesicles, macrocracks, and microcracks induced by impact, surface, and buried regolith layers, lava tubes will also contribute to the porosity of basalt [8]. The average thicknesses of the regolith layers are 4 ~ 5 m in maria. They are so small that the porosities contributed by them can be ignored. Lava tubes are rarely distributed throughout the Moon, and LRS surveys in unit H5 did not reveal changes corresponding with lava tubes. We expect that the porosity of the lunar basalts should be relatively constant, as it forms in a globally uniform manner. Based on Kiefer’s new porosity measurements using the bead method and helium pycnometry for Apollo samples and lunar meteorites, we use a value of 7% in this study [19]. After determining porosity, we can also determine the relationship between bulk density and grain density of basalt.

B. Determining Bulk Dielectric Constant

The grain density of lunar basalts can be calculated by the semiempirical formula summarized by Huang *et al.* [20]

$$\rho_{\text{grain}} = 0.0273\text{FeO} + 0.011\text{TiO}_2 + 2.773. \quad (9)$$

Based on Fa’s measurement and study of lunar soil samples, we can take the real part of the dielectric constant of lunar soil samples $\epsilon'_{\text{sample}} = 2.75$ and the density $\rho_{\text{sample}} = 1.7 \text{ g/cm}^3$. Fa *et al.* also summarized the relationship between the titanium content and the loss tangent of lunar soil when its density is

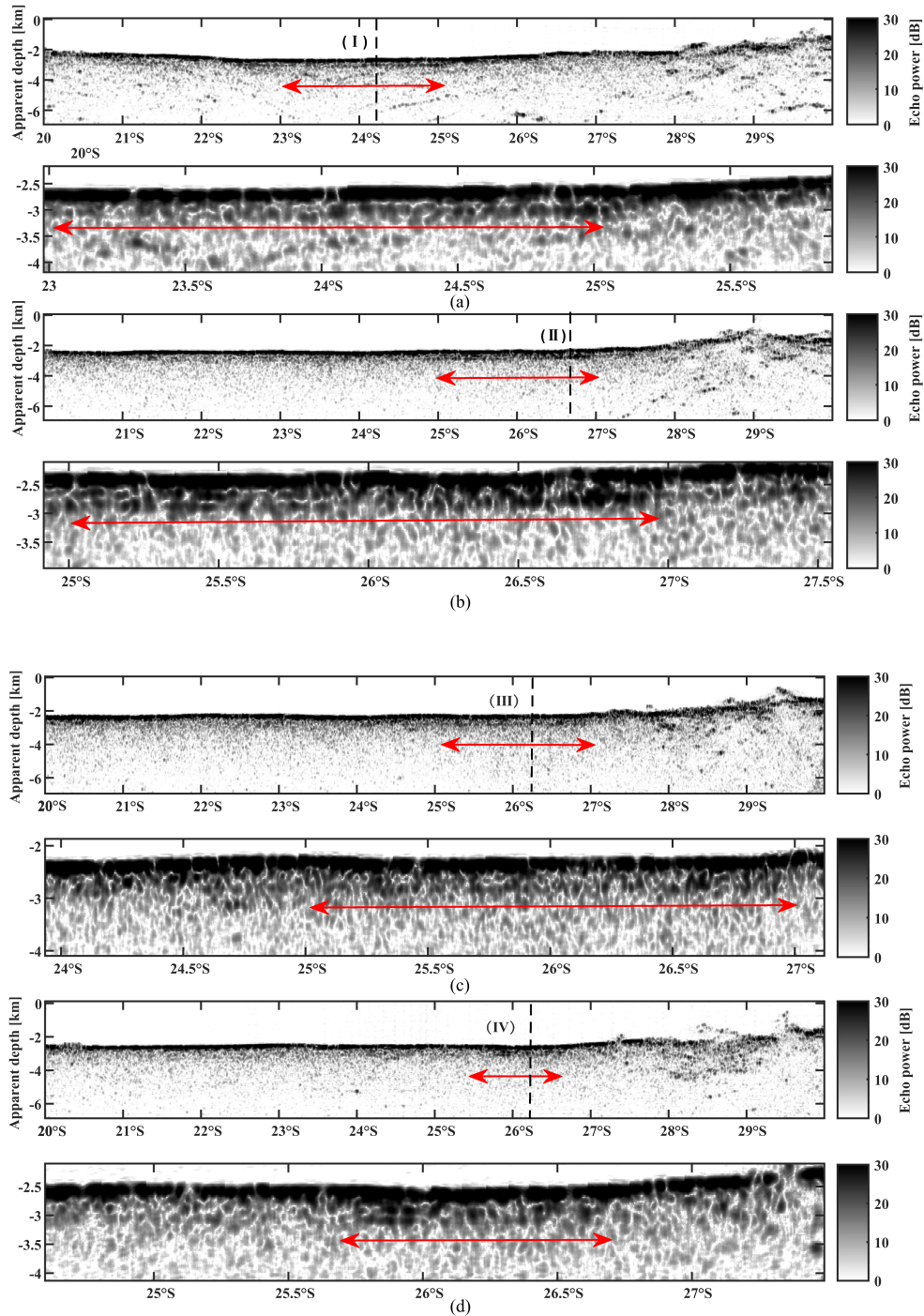


Fig. 3. B-scan of four LRS ground tracks (a)-(d) on unit H5 well reflect the subsurface feature of the region. Note that each radargram has its zoom version below it and reflectors are strong echoes which are parallel to surface echoes which are tagged by the red double-arrows. The black dotted line marked with Roman numerals is the A-scope data used to measure the thickness of the reflector, as shown in Fig. 5.

1.7 g/cm^3 , as follows [11]:

$$\log_{10}(\tan \delta) = -2.395 + 0.064 \text{TiO}_2 (\rho = 1.7 \text{g/cm}^3). \quad (10)$$

The dielectric constant of the lunar soil sample with the same titanium content as in the study area can be calculated by the following formula:

$$\varepsilon_{\text{sample}} = \varepsilon'_{\text{sample}} \cdot (1 + j \cdot \tan \delta). \quad (11)$$

We can get bulk density from 7% porosity and grain density. Then, the complex dielectric constant in bulk density is estimated using the Maxwell-Garnett mixing formula

$$\frac{1}{\rho_{\text{bulk}}} \cdot \frac{\varepsilon_{\text{bulk}} - 1}{\varepsilon_{\text{bulk}} + 2} = \frac{1}{\rho_{\text{sample}}} \cdot \frac{\varepsilon_{\text{sample}} - 1}{\varepsilon_{\text{sample}} + 2}. \quad (12)$$

Due to practical constraints, MI can only obtain FeO and TiO_2 content at a depth of $1 \mu\text{m}$ on the lunar surface. However, the

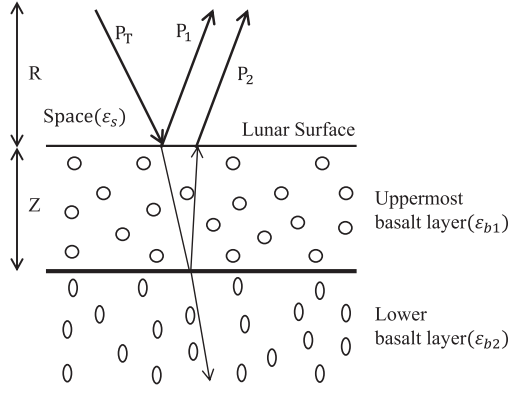


Fig. 4. Two-layer model adopted by this study. P_i is the incident wave, P_r is the surface reflected wave, P_2 is the subsurface reflected wave. R and Z are the height of the spacecraft and the depth of the reflector, respectively.

chemical composition of the lunar soil may be uniform for the influence of impact gardening on lunar soil remodeling [21]. If studying the chemical composition of basalt, it can be considered that the composition of basalt in the same period is consistent, so that the FeO and TiO₂ content of surface obtained by MI can represent the FeO and TiO₂ content of deep layer [22].

IV. ESTIMATING THE THICKNESS OF THE UPPERMOST BASALT LAYER

If apparent depth of reflector (d_{apparent}) and the real component of bulk dielectric constants (ϵ'_{bulk}) are known, this region's uppermost basalt layer thickness (equal to reflector's real depth) will be determined by the next formula

$$d_{\text{real}} = \frac{d_{\text{apparent}}}{\sqrt{\epsilon'_{\text{bulk}}}}. \quad (13)$$

This study uses LRS data to determine the apparent depth. B-scan datas are used to clarify the reflectors' locations in maria and A-scope datas are used to measure the distance between surface echo and subsurface echo in waveform of the LRS raw echo. Fig. 2 shows the four LRS ground tracks on unit H5. The LRS data of these four tracks are to estimate the approximate thickness of unit H5.

A. Two-Layer Model

Due to the significant differences in dielectric constants between vacuum and the uppermost layer of basalt, the uppermost layer and lower layer of basalt, LRS will get two strong echoes on the surface and the interface between the two layers of basalt. In the two-layer model, the incident wave is perpendicular to the surface. Fig. 4 illustrates this model. This model has a strong implicit assumption that the reflector is the weathering layer between the uppermost basalt and the lower basalt.

This model shows that the uncertainty in dielectric constant will directly affect any inversion attempt for the basalt layer thickness. Suppose that the true values of the complex dielectric constant and basalt layer thickness are $\epsilon_0 = \epsilon'_0 + i\epsilon''_0$ and d_0 , respectively. If the real component of the dielectric constant was incorrectly determined with uncertainties $\Delta\epsilon'_0$, then it is clear

that this would induce an uncertainty in the basalt layer thickness Δd_0 , according to

$$\frac{\Delta d_0}{d_0} = \sqrt{1 + \frac{\Delta\epsilon'_0}{\epsilon'_0}} - 1. \quad (14)$$

If we take as an example a 200 m thick basalt layer in the maria, a 10% uncertainty in the real component of the dielectric constant would cause a thickness inversion error of 4.8%, which is 9.7 m.

B. Basalt Layer Thickness Inversion

The basalt thickness of most lunar maria has been estimated using radar data. According to the previous research [4], clear continuous subsurface reflectors are detected only in a few areas from the B-scan data: Mare Humorum, Mare Imbrium, and Oceanus Procellarum. Unit H5 in Mare Humorum is older than 3.5Ga, which means that the basalt layer is more prone to stratification [4], and a single horizontal reflector is clearly detected in B-scan. Ishiyama *et al.* used the excavation depths of two types of craters (haloed and nonhaloed craters, the 1 and 2 in Fig. 2) to limit the basalt thickness in unit H5 to 213–300 m and to estimate the bulk dielectric constants to be 2.8–5.5 (see Table I). Oshigami *et al.* adopted the range of the value (2.8–5.5) as a relative permittivity of the unit H5, and estimated the actual depth of the reflector at 316.9°E, 20–28°S to be 220 m. However, the dielectric constant map (see Fig. 2) shows that impact craters 1 and 2 are located at a low-value area, where the dielectric constants are lower than other regions in unit H5. Therefore, the dielectric constants estimated by Ishiyama can not represent the overall situation of unit H5 and the actual depths estimated by Ishiyama and Oshigami *et al.* deviate from the true value and are too large.

Because the LRS orbit is a polar orbit, its ground track is almost parallel to the longitude in the image. For detection, we select one orbit respectively from east longitude 315, 316, 317, and 318. We observe its B-scan data and find out the subsurface reflector, which are marked by red double-arrow in Fig. 3. In order to simplify the research, this research focuses on laterally continuous subsurface reflectors. The off-nadir crater edge on the surface forms a curved reflector in the B-scan, whereas a straight line parallel to the surface is generally the subsurface boundary interface [23]. Since the reflector is parallel to the lunar surface, we can select A-scope data to measure the apparent depth at any point in the reflector. Here, we select the location of solid echo power in B-scan to extract A-scope, which is convenient for identifying surface and subsurface echoes and measure the apparent depth (as shown in Fig. 5). The apparent depths of four reflectors are 469, 468, 468, 327 m which are very close to that detected by Oshigami and Ishiyama *et al.* We divide the apparent depths by the square root of the dielectric constant represented by the white solid line in Fig. 2 and get the Fig. 6.

Previous research on basalt thickness assumed that the dielectric constant is single and does not change with longitude and latitude. The difference in this article is that we use the dielectric constant's spatial distribution to calculate the reflector's depth. In this way, the uppermost basalt layer of unit H5 in

TABLE I
SUMMARY OF THE DATA ANALYSIS

Regions	Reflector a	Reflector b	Reflector c	Reflector d	Oshigami's Research [4]	Ishiyama's Research [8]
Latitude	23-25°S	25-27°S	25-27°S	25.7-26.7°S	20-28°S	25.97°S,25.85°S
Longitude	315.753°E	316.987°E	317.786°E	318.191°E	316.9°E	316.65°E,316.73°E
Age(Ga)	3.53	3.53	3.53	3.53	3.53	3.53
ϵ_{bulk}	6.28-6.98	6.26-6.76	6.26-6.74	6.11-7.03	2.8-5.5	2.8-5.5
Porosity(%)	7	7	7	7	-	-
Apparent Depth(m)	469	468	468	327	480	500
Actual Depth(m)	177-190	180-187	180-187	123-132	150-310	214-300

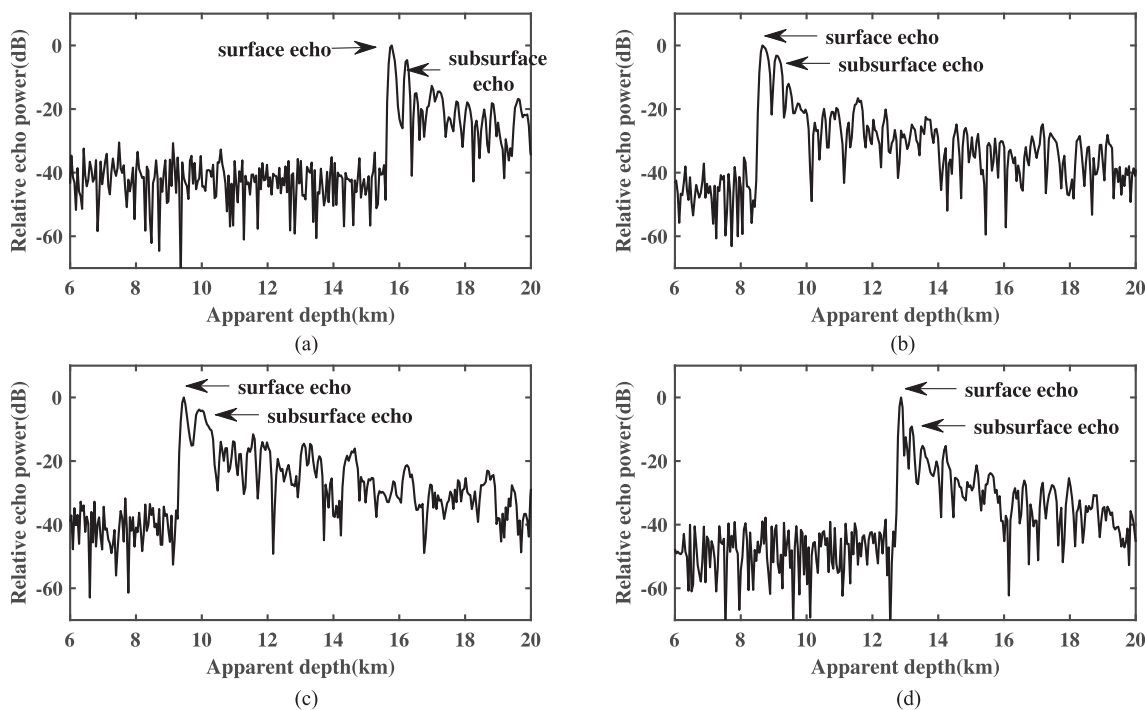


Fig. 5. A-scope data plot of LRS observation in Fig. 3. These data were acquired at (315.75°E, 24.00°S), (316.98°E, 26.53°S), (317.78°E, 26.00°S), (318.19°E, 26.00°S) in Mare Humorum. Arrows indicate nadir surface and subsurface echo peaks. (a) 24.000°S. (b) 26.533°S. (c) 26.001°S. (d) 26.001°S.

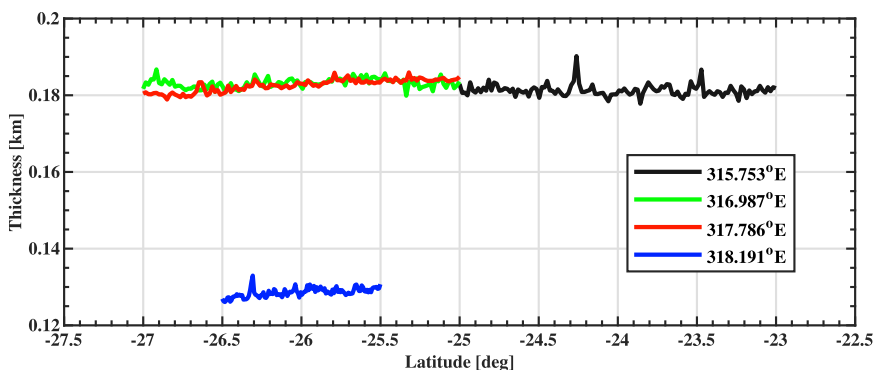


Fig. 6. Thickness of the reflector in Fig. 2. The transverse axis represents their spatial range, and the longitudinal axis represents the distance between the reflector and the lunar surface, i.e., the thickness of the topmost basalt.

Mare Humorum can be observed more intuitively, as shown in Fig. 6. The basalt thickness of unit H5 is about 180 m, with no more than 10 m variations, except the southeastern part (318°E, 25.5 – 26.5°S) is only 123–132 m thick. The southeast part of unit H5 is adjacent to units H6 and H7. Basalt of units H6 and H7 may intrude below the boundary of unit H5, resulting in a thinner basalt layer than other parts.

V. CONCLUSION

Based on the estimated FeO and TiO₂ content distribution and the assumed maria basalt porosity, we use Maxwell–Garnett theory to determine the unique dielectric constant values of unit H5. Using the two-layer model and radar range equation to calculate the thickness of basalt, we find that the thickness of upper basalt in unit H5 is 180 and 120 m at the border between unit H5 and H7.

Nevertheless, this thickness inversion method has many uncertain factors. In our dielectric constant map, the low penetration of MI spectrum data could lead to uncertainties in dielectric constant of the uppermost basalt layer. The method is still more advanced than previous research, although some physical quantities contain uncertainties. Its inversion of the dielectric constant is better.

Finally, more *in situ* detection, more advanced measurement equipment and more well-designed models are needed for the future research on maria basalt.

ACKNOWLEDGMENT

The authors would like to thank Dr. Wenzhe Fa from Peking University for his comments and contribution to the early versions of this manuscript.

REFERENCES

- [1] J. Du, W. Fa, M. A. Wicczorek, M. Xie, Y. Cai, and M.-H. Zhu, “Thickness of lunar mare basalts: New results based on modeling the degradation of partially buried craters,” *J. Geophys. Res., Planets*, vol. 124, no. 9, pp. 2430–2459, 2019. [Online]. Available: <https://agupubs.onlinelibrary.wiley.com/doi/abs/10.1029/2018JE005872>
- [2] J. W. Head, “Lunar mare deposits: Areas, volumes, sequence, and implication for melting in source areas,” *LPI Contributions*, vol. 234, 1975, Art. no. 66.
- [3] T. Ono *et al.*, “Lunar radar sounder observations of subsurface layers under the nearside maria of the moon,” *Science*, vol. 323, no. 5916, pp. 909–912, 2009.
- [4] S. Oshigami *et al.*, “Mare volcanism: Reinterpretation based on KAGUYA lunar radar sounder data,” *J. Geophys. Res., Planets*, vol. 119, no. 5, pp. 1037–1045, 2014.
- [5] W. J. Peeples *et al.*, “Orbital radar evidence for lunar subsurface layering in maria serenitatis and crisium,” *J. Geophys. Res., Solid Earth*, vol. 83, no. B7, 1978, Art. no. 3459.
- [6] B. L. Cooper, J. L. Carter, and C. A. Sapp, “New evidence for graben origin of oceanus procellarum from lunar sounder optical imagery,” *J. Geophys. Res. Atmos.*, vol. 99, no. E2, pp. 3799–3812, 1994.
- [7] S. Oshigami *et al.*, “Distribution of the subsurface reflectors of the western nearside maria observed from KAGUYA with lunar radar sounder,” *Geophys. Res. Lett.*, vol. 36, no. 18, pp. 252–260, 2009.
- [8] K. Ishiyama *et al.*, “Estimation of the permittivity and porosity of the lunar uppermost basalt layer based on observations of impact craters by selene,” *J. Geophys. Res., Planets*, vol. 118, no. 7, pp. 1453–1467, 2013.
- [9] K. Hongo, H. Toh, and A. Kumamoto, “Estimation of bulk permittivity of the Moon’s surface using lunar radar sounder on-board selenological and engineering explorer,” *Earth, Planets Space*, vol. 72, no. 1, pp. 1–15, 2020.
- [10] Y. Bando, A. Kumamoto, and N. Nakamura, “Constraint on subsurface structures beneath reiner gamma on the moon using the KAGUYA lunar radar sounder,” *Icarus*, vol. 254, pp. 144–149, 2015.
- [11] W. Fa and M. A. Wicczorek, “Regolith thickness over the lunar nearside: Results from earth-based 70-cm Arecibo radar observations,” *Icarus*, vol. 218, no. 2, pp. 771–787, 2012.
- [12] W. D. Carrier I, G. R. Olhoeft, and W. Mendell, “Physical properties of the lunar surface,” in *Lunar Sourcebook, A User’s Guide to the Moon*, G. H. Heiken, D. T. Vaniman, and B. M. French, Eds., 1991, pp. 475–594.
- [13] H. Hiesinger, J. W. Head, U. Wolf, R. Jaumann, and G. Neukum, “Lunar mare basalt flow units: Thicknesses determined from crater size-frequency distributions,” *Geophys. Res. Lett.*, vol. 29, no. 8, pp. 89–1–89-4, 2002.
- [14] G. R. Olhoeft and D. W. Strangway, “Dielectric properties of the first 100 meters of the moon,” *Earth Planet. Sci. Lett.*, vol. 24, no. 3, pp. 394–404, 1975.
- [15] Y. G. Shkuratov and N. V. Bondarenko, “Regolith layer thickness mapping of the moon by radar and optical data,” *Icarus*, vol. 149, no. 2, pp. 329–338, 2001.
- [16] P. G. Lucey, D. T. Blewett, and B. L. Jolliff, “Lunar iron and titanium abundance algorithms based on final processing of clementine UV-visible images,” *J. Geophys. Res. Planets*, vol. 105, no. E8, pp. 20297–20305, 2000.
- [17] M. Lemelin, P. G. Lucey, E. Song, and G. J. Taylor, “Lunar central peak mineralogy and iron content using the KAGUYA multiband imager: Re-assessment of the compositional structure of the lunar crust,” *J. Geophys. Res. Planets*, vol. 120, no. 5, pp. 869–887, 2015.
- [18] H. Otake, M. Ohtake, and N. Hirata, “Lunar iron and titanium abundance algorithms based on SELENE (KAGUYA) multiband imager data,” in *Proc. 43rd Lunar Planet. Sci. Conf.*, Mar., 2012, p. 1905.
- [19] W. S. Kiefer, R. J. Macke, D. T. Britt, A. J. Irving, and G. J. Consolmagno, “The density and porosity of lunar rocks,” *Geophys. Res. Lett.*, vol. 39, no. 7, 2012, Art. no. 7201.
- [20] Q. Huang and M. A. Wicczorek, “Density and porosity of the lunar crust from gravity and topography,” *J. Geophys. Res. Atmos.*, vol. 117, no. E5, 2012.
- [21] E. S. Costello, R. R. Ghent, M. Hirabayashi, and P. G. Lucey, “Impact gardening as a constraint on the age, source, and evolution of ice on mercury and the moon,” *J. Geophys. Res., Planets*, vol. 125, no. 3, 2020, Art. no. e2019JE006172.
- [22] H. J. Melosh, *Planetary Surface Processes*, vol. 13. Cambridge, U.K.: Cambridge Univ. Press, 2011.
- [23] T. Ono *et al.*, “Instrumentation and observation target of the lunar radar sounder (LRS) experiment on-board the SELENE spacecraft,” *Earth, Planets, Space*, vol. 60, pp. 321–332, 2008.